Published in final edited form as:

Oncogene. 2018 July ; 37(28): 3778–3789. doi:10.1038/s41388-018-0241-0.

Inhibition of ovarian tumor cell invasiveness by targeting SYK in tyrosine kinase signaling pathway

Yu Yu[1,2], **Yohan Suryo Rahmanto**[1,2], **Meng-Horng Lee**[3], **Pei-Hsun Wu**[3], **Jude M. Phillip**[3], **Chuan-Hsiang Huang**[2], **Michele I. Vitolo**[4], **Stephanie Gaillard**[1,5], **Stuart S. Martin**[4], **Denis Wirtz**[3], **Ie-Ming Shih**[1,2,5], and **Tian-Li Wang**[1,2,5]

[1]Sidney Kimmel Comprehensive Cancer Center, Johns Hopkins Medical Institutions, Baltimore, MD 21205, USA

[2]Department of Pathology, Johns Hopkins Medical Institutions, Baltimore, MD 21287, USA

[3]Department of Chemical and Biomolecular Engineering, Physical Sciences-Oncology Center, and Institute for NanoBioTechology, Johns Hopkins University, Baltimore, MD 21218, USA

[4]Department of Physiology, University of Maryland School of Medicine, Baltimore, MDMarlene and Stewart Greenebaum National Cancer Institute Cancer Center, University of Maryland School of Medicine, Baltimore, MD 21201, USA

[5]Gynecology and Obstetrics, Johns Hopkins Medical Institutions, Baltimore, MD 21287, USA

Abstract

Ovarian cancer cell motility and invasiveness are prerequisites for dissemination, and largely account for cancer mortality. We have identified an actionable kinase, spleen tyrosine kinase (SYK), which is keenly associated with tumor progression in ovarian cancer. Here, we report that active recombinant SYK directly phosphorylates cortactin and cofilin, which are critically involved in assembly and dynamics of actin filament through phosphorylation signaling. Enhancing SYK activity by inducing expression of a constitutively active SYK mutant, SYK^{130E}, increased growth factor-stimulated migration and invasion of ovarian cancer cells, which was abrogated by cortactin knockdown. Similarly, SYK inhibitors significantly decreased invasion of ovarian cancer cells through basement membrane matrix in a real-time transwell assays and in a 3-D tumor spheroid model. SYK inactivation by gene knockout or by small molecule inhibition reduced actin polymerization. Collectively, the results reported here identify a new mechanism by which SYK signaling regulates ovarian cancer cell motility and invasiveness, and pinpoint a target-based strategy to prevent or suppress the advancement of ovarian malignancies.

Correspondence: Professor Ie-Ming Shih, Department of Gynecology and Obstetrics, Johns Hopkins Medical Institutions, 1550 Orleans Street, CRB2 RM 305, Baltimore, MD 21231, USA, shihie@yahoo.com; Professor Tian-Li Wang, Department of Pathology, School of Medicine, Johns Hopkins University, 1550 Orleans Street, CRB2 RM 306, Baltimore, MD21231, USA, tlw@jhmi.edu.

Conflict of interest

The authors declare no potential conflicts of interest.

Keywords

ovarian cancer; phosphoproteomics; spleen tyrosine kinase; cell invasion; F-actin dynamics

Introduction

Acquisition of motility and invasiveness during tumor evolution are essential for cancer dissemination and metastasis. Developing these new features endows tumor cells with the ability to dissociate and migrate out of the primary tumor, perhaps in response to environmental cues, and to invade the surrounding normal tissue and angiolymphatic space.[1] Cancer cell motility in response to environmental stimuli is a highly-regulated process that involves sensing of chemical signals in the environment and transmission of the signals to initiate and regulate the polarized assembly of actin filaments.[2] Although the biophysical properties of actin subunit assembly have been well-studied, how environmental cues trigger nucleation and polarized assembly of actin filaments in the tumor cell context remains poorly understood.[3–7]

To date, genome-wide analyses have revealed the molecular landscapes of major types of primary human cancers; however, there remain a lack of therapeutic actionable targets for preventing or controlling metastasis. One approach that may expedite the discovery and clinical relevance of such molecules would be to identify and characterize kinases that regulate polarized assembly of actin filament in motile cells, and to clinically evaluate readily available, small compound inhibitors to target these kinases. In a recent proteomic analysis, we identified spleen tyrosine kinase (SYK) overexpression in recurrent ovarian cancers, and found that SYK expression was associated with a less favorable chemo-response to paclitaxel/platinum-based combination therapy.[8] Importantly, SYK has been implicated in the actin dynamics pathway, as several of its kinase substrate proteins are involved in modifying the actin cytoskeleton.

SYK is a non-receptor tyrosine kinase that mediates signal transduction of cellular transmembrane receptors, including immunoreceptors and integrins.[9] Upon activation of these receptors through ligand binding, e.g., antigen on B cell receptor, the receptor-associated SRC family kinases in proximity to SYK phosphorylate SYK at Tyr525 and Tyr526 in the activation loop of the kinase domain, resulting in enzymatic activation of SYK.[10, 11] Activated SYK signaling is essential for tumor cell proliferation and survival in B-cell malignancies.[12, 13] The pro-survival functional role of SYK in cancers of epithelial origin are also beginning to be recognized.[14–17] SYK can be targeted through inhibition of its enzymatic activity, and importantly, orally active SYK inhibitors Fostamatinib (R788, prodrug of R406) and entospletinib (GS-9973) have been tested in clinical studies for treatment of rheumatoid arthritis and hematological malignancies.[18–21] These compounds are relatively safe, with mild but reversible side effects in patients. The availability of clinical-grade inhibitors would facilitate the translation of SYK target-based therapy in ovarian cancer patients. With these considerations in mind, this study was undertaken to elucidate the function of SYK in promoting tumor advancement, and to test the capacity of

pharmacological inhibition of SYK signaling to prevent or suppress the tumor progression processes.

Results

Active SYK promotes migration and invasion of ovarian cancer cells induced by epithelial growth factor

To examine the phenotypic consequence of SYK activation in human tumor cells, we established a Tet-Off tetracycline-regulated gene expression system in an ovarian cancer cell line, SKOV3, which displays low endogenous SYK expression.[8] The system permits expression of the constitutively active SYK mutant, SYK^{130E}, under tight temporal control of doxycycline, a derivative of tetracycline.

Migration assays started 48 h after the removal of doxycycline, a point at which SYK^{130E} expression was evident from a GFP tracking signal. Growth factor (EGF)-induced motility was monitored using a live-cell time-lapse imaging system. Induced expression of SYK^{130E} (−Dox) resulted in more cells migrating toward increasing growth factor concentration (Figure 1A), but did not affect velocity of movement compared to non-induced cells (+Dox) (Supplementary Figure 1A). Movements of SYK-expressing cells were more directed, as reflected by significant increases in the calculated directness index (Figure 1B, $p=0.0021$) and in the x-axis Forward Migration Index (xFMI) (Figure 1C, $p<0.0001$). These data suggest that the presence of active SYK in the tumor cells stimulates the activation of directed motility, a phenotype frequently associated with invasive tumors.

Next, we assessed whether inhibition of SYK by a small molecular tyrosine kinase inhibitor, R406, blocked chemotaxis induced by growth factor. Based on the trajectories of the imaged cells, it was evident that R406 markedly reduced cell motility and displacement of SKOV3 cells from their original locations (Figure 1D). Calculated parameters from these trajectories indicated that R406 treatment significantly reduced the velocity of the cells (Figure 1E, $p<0.001$), and reduced the accumulated distance traveled (Supplementary Figure 1B, $p<0.001$). Furthermore, the addition of R406 to SKOV3 cells with induced expression of SYK^{130E} abrogated EGF-induced directional movement (Supplementary Figure 2A). The calculated xFMI, cell movement velocity, and accumulated migration distance were concomitantly decreased (Supplementary Figure 2B, $p<0.002$).

We also assessed the potency of invasion in SKOV3 tumor cells with or without induced SYK^{130E} expression using an electrical impedance-based technique, which performs real-time monitoring and quantification of EGF-induced tumor cell invasion through the extracellular matrix-coated gold microelectrode array. As cells attach and spread on the electrode surface, electron flow at the electrode-solution interface is impeded. The magnitude of impedance is displayed as delta cell-index, reflecting the number of cells invading through the extracellular matrix. In the presence of EGF, active SYK^{130E}-expressing mutants exhibited an increased rate of cell invasion compared to cells without induced SYK^{130E} expression (Figure 2A, $p<0.001$). In contrast, in the absence of EGF, ectopic SYK^{130E} expression did not lead to increased cell invasion, suggesting that active SYK-mediated invasive behavior is dependent on EGF (Figure 2A). Moreover, inhibition of

SYK signaling by R406 significantly blocked EGF-induced invasion (Figure 2B, $p<0.001$). We also examined wild-type SYK (SYK^{WT}) under the same Tet-Off expression system, and showed that consistent with data obtained from the kinase active 130E mutant, ectopic SYK^{WT} expression also increased the degree of cell invasion, although to a lesser extent compared to the changes observed in the SYK^{130E} cells (Supplementary Figure 3A).

SYK directly phosphorylates cortactin and cofilin-1, and SYK inhibition reduces cortactin phosphorylation and tumor invasion in spheroid models

In a previous SILAC-based proteomic study, we found that actin-associated proteins, cortactin (CTTN) and cofilin (CFL1) were potential substrates of SYK.[8] Both cortactin and cofilin are actin-binding proteins that participate in promoting actin nucleation and assembly during cell motility, and have a central role in the development and maturation of invadopodia, which are actin-driven protrusive structures in invasive cancer cells that degrade the extracellular matrix.[22–25] Therefore, we tested whether these two actin-associated proteins were directly phosphorylated by SYK. In vitro kinase assays were performed by incubating recombinant SYK protein with its potential substrate protein. We observed that SYK readily phosphorylates cortactin (CTTN, Figure 2C) and cofilin (CFL1, Figure 2D) in the presence of ATP, as detected using an antibody specific for phosphotyrosine. Moreover, by measuring the conversion (consumption) rate from ATP to ADP in these kinase reactions, we found a linear increase in ADP production concomitant with the increased amounts of phosphorylated cortactin and cofilin (Figure 2E and 2F).

Inhibition of SYK by three different SYK inhibitors, R406, Entospletinib, and GS9876, all reduced pCTTN (Y421) in ovarian cancer cells (Figure 3A). In a complementary study, in SKOV3 cells with induced expression of SYK^{130E}, we found a concomitant increase in cortactin phosphorylation on Y421 (Figure 3B). SYK^{WT} induction also increased levels of pCTTN (Y421), although to a lesser extent compared to the levels in SYK^{130E} expressing cells (Supplementary Figure 3B). We were unable to perform a similar experiment for phospho-cofilin because of the lack of an appropriate phosphotyrosine site-specific antibody. In SKOV3 SYK^{130E} cells, siRNA-mediated knockdown of CTTN (Figure 3C–3E) or CFL1 (Figure 3C and 3F) suppressed their invasive capacity, further highlighting the role of active SYK in mediating EGF-induced invasion through CTTN and CFL1.

Next, we examined SYK inhibitor (R406) in a 3-dimensional cell culture system using collagen matrix-embedded tumor spheroids derived from the ovarian cancer cell lines SKOV3 and OVISE (Figure 4A and 4B). R406 treatment significantly reduced the number of radially invading cells in both the SKOV3 model (Figure 4A and 4C) and the OVISE model (Figure 4B and 4D). R406 treatment did not significantly affect proliferation of SKOV3 (Figure 4E) or OVISE (Figure 4F) cells in the tumor spheroid cultures, excluding the possibility that the decrease in cell invasion was due to reduced cellular proliferation. In contrast to SYK inhibition, induced expression (–Dox) of SYK^{130E} active mutant in spheroid cultures resulted in increased invasiveness compared to SKOV3 cells without induced expression of SYK^{130E} (+Dox) as quantitated by measuring Hoechst33342 fluorescent intensity of invading cells (Supplementary Figures 4A and 4B).

SYK activity affects cortical F-actin intensity

To further understand the mechanism of invasion promoted by activated SYK, we examined the localization of pSYK (Y525/526), a surrogate of active SYK, in OVISE ovarian cancer cells, which express a relatively high level of endogenous SYK.[8] We found that pSYK immunofluorescence signals co-localized with F-actin (Figure 5A), raising the possibility that pSYK enzymatic activity may regulate actin and/or actin-associated proteins. Because SYK co-localized with F-actin and promotes cortactin and cofilin phosphorylation, we examined whether changes in SYK expression levels or kinase activity would alter F-actin staining intensity, architecture, and distribution in cells. Both SYK knockout and ectopic expression models were employed. SYK knockout markedly reduced F-actin intensity and disassociated cortical F-actin compared to SYK wild-type cells (Figure 5A), while ectopic expression of the constitutively active SYK^{130E} mutant (−Dox) led to a prominent F-actin structure (Figure 5B). To corroborate this finding, we examined cell populations on a high-throughput cell imaging platform (htCIP) using a previously reported method.[26] This method permits the rapid extraction of high-content information from individual cells, including cellular and nuclear morphology. The assay also provides accurate intensity measurements at the single-cell level. F-actin staining intensity was reduced in OVISE SYK knockout cells in comparison to the wild-type cells which express endogenous levels of SYK (Figure 5C and Supplementary Figure 5A). Treatment of $SKOV3^{TR}$ and $MPSC1^{TR}$ ovarian cancer cells with SYK inhibitor (R406 or Entospletinib) phenocopied the SYK knockout (Figure 5D and Supplementary Figure 5B). The $SKOV3^{TR}$ and $MPSC1^{TR}$ paclitaxel resistant cells were used in these experiments because of the high endogenous SYK expression relative to their parental counterparts.[8] Furthermore, serum starvation of cells overexpressing active SYK^{130E} mutant resulted in higher F-actin intensity than cells without SYK^{130E} induction (Figure 5E and 5F).

We also performed confocal image analysis of F-actin staining and SYK^{130E}-GFP on the SKOV3 spheroid cultures with induced expression of SYK^{130E}-GFP and found that F-actin filament and SYK^{130E}-GFP signals at the invasive edge of the spheroid were co-localized (Supplementary Figure 4A–C). To understand localization/organization of SYK and cortactin, we also performed pSYK (Y525/526) and pCTTN (Y421) immunohistochemistry on the formalin-fixed paraffin-embedded SKOV3 spheroid cultures. The staining of pSYK (Y525/526) and pCTTN (Y421) were pronounced and co-localized at the periphery and invasive protrusion structures of SKOV3 spheroids with induced SYK^{130E} expression (−Dox). On the other hand, diffuse staining of pSYK and pCTTN were found in SKOV3 spheroid cultures without induced SYK^{130E} expression (+Dox) (Supplementary Figure 4D).

SYK affects EGF-induced polarized actin assembly

Actin leading edge protrusion depends on continuous actin nucleation and assembly as the initial step to navigate and promote directional cell migration.[27] In this study, we assessed whether SYK mediates actin leading edge protrusion using Total Internal Reflection Fluorescence (TIRF) microscopy to image ovarian cancer cells transfected with LifeAct-RFP as a biosensor for F-actin.[28, 29] This technique allows visualization of cytoskeletal dynamics on the basal plasma membrane of the cell. We analyzed fluorescence images and calculated the protrusion dynamics in isogenic pairs of OVISE SYK^{KO} and SYK^{WT} cells in

the presence of the motility stimulant, EGF (Supplementary video 1–3). While OVISE SYK^{WT} cells expressed endogenous levels of SYK, SYK expression in the OVISE SYK^{KO} cells was completely eliminated (Supplementary Figure 5A). Although the cell adherent area remained stable in unstimulated cells, EGF stimulation caused a rapid increase in adherent area in OVISE SYK^{WT} cells and to a lesser extent in OVISE SYK^{KO} cells (Figure 6A, $p<0.001$). R406, a SYK inhibitor, largely suppressed the EGF-stimulated effect in wild-type cells. On the other hand, SYK^{130E} expression caused a rapid increase in cell area upon EGF stimulus in comparison to cells without SYK^{130E} expression (Figure 6B, $p<0.001$, 6C, and supplementary video 4–6). The effect of SYK^{130E} expression was reduced by R406 treatment. Furthermore, CTTN knockdown also reversed the effect of SYK^{130E} as compared to control siRNA transfected cells (Figure 6D, $p<0.001$). These data suggest that CTTN is an important mediator of the effect of active SYK in modulating actin cytoskeleton.

Discussion

This study describes a new role for the SYK signaling pathway in promoting directional cancer cell migration and invasion, a fundamental step in cancer dissemination and metastasis. Upon growth factor stimulus, SYK mediated a serial biochemical event including alterations in the assembly and dynamics of actin filaments and formation of polarized actin protrusion filaments. Our results showed that two of the actin-associated proteins, cortactin and cofilin, which involved in cell movement were directly phosphorylated by SYK. Additionally, SYK inhibition resulted in reduced cell motility and reduced invasion in tumor spheroid models at a concentration of inhibitor that did not affect cell viability or cell growth. Collectively, our results support future investigation to evaluate clinical-grade SYK inhibitors for treating advanced cancers.

As a non-receptor tyrosine kinase in normal cells, SYK signaling can be triggered by environmental stimuli, e.g., pro-inflammatory signals and extracellular matrix, through an interaction with cell membrane receptors including B cell receptors and integrins.[9] However, it is still unclear which environmental cues stimulate SYK signaling in malignant cells. Our data showing that EGF growth factor potently stimulated SYK-mediated directional migration and invasion in cancer cells indicates that, in human malignancies, SYK may be one of the key cellular meditators responding to changes in tumor microenvironment. Therefore, future studies are needed to identify environmental factors, such as growth factors and cytokines, which may trigger SYK signaling in cancer cells.

The SYK phosphorylation sites in cortactin and cofilin have been identified previously, and can be regulated by other kinases.[22–25, 30] These specific phosphorylation sites in cortactin and cofilin are critical for cell motility, operating through actin dynamic modification and filament assembly.[24, 25] Considering the role of cortactin and cofilin in actin regulation, and the effect that tyrosine phosphorylation of these two proteins has on cell migration status, [24, 25] all the data point to a functional role of SYK in regulating cell migration, likely through direct phosphorylation of cortactin and cofilin. Although SYK-mediated phosphorylation of cortactin and cofilin is our preferred interpretation of the observed SYK activity on cell motility and invasion, other potential mechanisms should also be considered. For example, SYK may phosphorylate an F-actin binding protein, SWAP-70, in B cells,

which regulates migration through direct interaction with Rho GTPase.[31, 32] Moreover, the PI3K pathway, which mediates chemotaxis in *Dictyostelium* and mammalian cells, may crosstalk with the SYK signaling pathway. This possibility is supported by the fact that components of PI3K signaling including p85 and PIK3R1 are potential kinase substrates of SYK.[8, 33–36] Collectively, our study suggests that SYK may interact with Rho and PI3K pathways to coordinately regulate actin cytoskeleton, cell polarity, and cellular movement. We noted that SKOV3 cells used in this study overexpress ErbB2 receptor,[37] a member of the EGFR family. ErbB2 receptor can interact with EGFR to form functional heterodimers on the cell membrane and respond avidly to EGF ligand.[38, 39] The EGF-stimulated motility and other aggressive behaviors as observed in SKOV3 cells may be attributable to their over-expression of ErbB2.

It is well-recognized that in B lymphocytes, which highly express SYK, the SYK pathway drives cell motility, polarization, and entry into lymph nodes [31] upon immunoreceptor stimulation.[40] It has also been shown that SYK inhibition redistributes the actin cytoskeleton in macrophages.[41] Based on our studies and those reported earlier on breast, head and neck, nasopharyngeal, and prostate cancers,[14, 15, 42, 43] the role of SYK in tumor invasion appears to be context and cell type-specific. In breast cancers, SYK mediated an anti-metastatic function as reduced SYK expression was associated with breast tumors with distant metastases, and its re-expression in highly malignant breast cancer cell lines was sufficient to suppress tumor growth, lung metastases and cell motility.[42,44] In contrast, re-expression of SYK in a SYK-negative head and neck squamous cancer cell line stimulated chemotaxis, while its inhibition in head and neck squamous cancer cells with high endogenous levels of SYK reduced chemotaxis.[14] High SYK expression was correlated with worse overall survival in patients with head and neck squamous carcinomas.[14] The pro-metastatic function of SYK has also been implicated in prostate cancer, where SYK kinase promoted metastatic dissemination in animal models of prostate cancers.[43] In Epstein-Barr virus (EBV) positive nasopharyngeal carcinomas, SYK was shown to be a substrate of an EBV viral protein, Latent Membrane Protein 2A (LMP2A), which induces constitutive activation of SYK and stimulates cell migration, and in the meantime, accelerates its protein turnover rate.[15]

The double edge sword of SYK function, being anti-metastatic in breast cancer while pro-invasive in ovarian cancer, head and neck, nasopharyngeal, and prostate cancers indicate the cell type-specific and context-dependent functional roles of SYK. The biphasic actions could be explained by unique intracellular adaptor molecules and substrates of SYK, as well as expression of specific cell surface receptors that trigger SYK signaling in different types of human carcinomas. It is worth noting that SYK has been found to be associated with EGFR in breast cancer, squamous cell carcinoma of the head and neck, as well as in ovarian cancer; however, its relationship with EGFR signaling appears to be contradictory. In breast epithelial cells, SYK appears to act as a negative regulator of EGFR signaling,[45] while in head and neck carcinoma [14] and in our current study of ovarian carcinoma, SYK acts a positive mediator of EGFR signaling, which potently stimulates motility and invasion of these two types of tumors. Since EGFR signaling plays a major regulatory role in tumor cell migration and invasion, the seemingly contradicting behaviors of SYK in different carcinomas may relate to variation in its crosstalk with EGFR. This line of observation

highlights the importance of future studies to evaluate crosstalk between EGFR and SYK signaling pathways in ovarian cancers.

We propose that SYK could serve as a potential molecular target for therapy because inactivation of SYK by small compound inhibitors simultaneously inhibits several signaling pathways critical for cancer cell migration and invasion. Our previous studies showed that SYK is upregulated in post-chemotherapy recurrent ovarian high-grade serous and clear cell carcinomas compared to primary tumors, and that SYK inhibition sensitizes paclitaxel cytotoxicity.[8] Ovarian high-grade serous carcinoma and clear cell carcinoma are the two most aggressive types of ovarian cancer, and both are associated with poor prognosis.[46] A more effective therapy is needed to delay tumor progression in patients with advanced disease. Currently, there are two SYK inhibitors, Fostamatinib (prodrug of R406) and Entospletinib (GS-9973), with favorable safety profiles in clinical trials for rheumatoid arthritis, non-Hodgkin lymphoma and chronic lymphocytic leukemia patients.[18–21, 47] Our data suggest that SYK kinase is a potential therapeutic target in ovarian cancer to reduce disease invasiveness. Repurposing these clinical-grade SYK inhibitors maybe useful in treating advanced malignancies where SYK signaling have been shown to promote cancer cell motility and invasion.

Materials and Methods

Cell lines and cell culture

Our previous study, which characterized total SYK expression levels using immunoblotting, identified several ovarian cancer cell lines with detectable total SYK expression. SKOV3 was obtained from the American Tissue Culture Center (Rockville, MD, USA). The MPSC1 cell line was previously described.[48] OVISE was obtained from the Japanese Health Science Research Resources Bank (Osaka, Japan). All cell lines were cultured in RPMI-1640 medium supplemented with 10% (v/v) fetal bovine serum and 1% penicillin/streptomycin. SKOV3 cells expressing SYK (active mutant 130E) under the Tetracycline-Off (Tet-Off) inducible system were generated as previously described.[8] The short tandem repeat (STR) DNA profiling of SKOV3 and OVISE cell lines were confirmed against Cellosaurus ExPASy database. SKOV3^{TR}, MPSC1^{TR}, SKOV3 SYK^{130E}, and OVISE SYK^{KO} were authenticated as isogenic to their respective parental cell lines using STR DNA analyses. SKOV3 SYK^{130E}, OVISE SYK^{WT}, and OVISE SYK^{KO} were tested negative for mycoplasma. The inducible cells were maintained in the presence of 1–2 μg/mL doxycycline to maintain the off condition preventing SYK expression. Doxycycline was removed from the medium to activate SYK expression as necessary.

Immunoblotting and Generation of SYK knockout OVISE cells

Equal amounts of protein preparations (15–30 μg of total cell lysate, and cytosolic, nuclear, and/or other fractions) were resolved on SDS-PAGE. The antibodies used include: anti-SYK (Abcam, Cambridge, United Kingdom, #ab3113), anti-pCTTN (Y421) (Millipore, #AB3852), anti-cortactin (Cell Signaling Technology, #3503), anti-pSYK (Y525/526) (Cell Signaling Technology, #2710), anti-cofilin (Abcam, #ab11062), anti-GFP (Clontech, #632375), anti-GAPDH (Sigma-Aldrich, St, Louis, MO, USA, #G9545), anti-mouse HRP

(Jackson Immuno Research, West Grove, PA, USA, #715-035-150), and anti-rabbit HRP (Jackson Immuno Research, #711-035-152). GAPDH was used as a loading control. The pSpCas9n(BB)-2A-Puro (PX462) CRISPR/Cas9 vector from Addgene (plasmid no. 48141) was used in this study. Cloning was performed using a pair of CRISPR single-guide RNA (sgRNA) specifically targeting exon 2 of SYK; top strand-nicking sgRNA (CGGACAGGGCGAAGCCACCC) and bottom strand-nicking sgRNA (CACACCACTACACCATCGAG) were designed and cloned as previously described.[49] OVISE cells were transfected using Lipofectamine® 3000 (Thermo Fisher Scientific), and positive cells were selected in the presence of 2 μg/ml puromycin. Single cell clones were isolated and screened for Cas9 expression. The SYK knock-out was verified by immunoblotting. Early passage (less than 3) knockout cells were used for experiments.

Cell Migration and xCELLigence Cell invasion Assays

Both parental SKOV3 and Tet-off inducible SKOV3 cells were re-suspended at 3×10^5 cells/100 μl and seeded onto chemotaxis μ-slides coated with collagen IV (Ibidi GmbH, Munich, Germany). The slide chamber was then flushed with serum-free medium, and the reservoirs on one side were filled with serum-free medium and on the other side with serum-free medium containing EGF (100 ng/mL). Live-cell imaging was performed using a Nikon Eclipse TE300 microscope (Nikon, Melville, NY, USA). Data were captured using a Hamamatsu ORCA-ER camera running SimplePCI automated image capture software (Hamamatsu Photonics, Hamamatsu, Japan). Cells were imaged at regular intervals (10 min) at 10× magnification for up to 24 h. Cell migration was manually tracked using CellTracker software and analyzed using ImageJ 'Chemotaxis and Migration Tool' plug-in. At least 30 cells that did not undergo division during the experiment were tracked per sample for adequate statistical analysis. Trajectory plots and various chemotactic responses were measured.

Chemotactic cell invasion was determined using the xCELLigence system (ACEA Biosciences, San Diego, CA, USA). For invasion studies, CIM-plate 16 were pre-coated using growth factor reduced Matrigel (800 μg/mL), medium containing EGF (25 ng/mL) was added to the lower chambers, and SKOV3 Tet-off inducible cells (30,000 cells/well in 1% FBS containing medium) were seeded in the upper inserts. Cells were serum starved for 10 h prior to the experiment. In the R406-treated group, cells were pre-treated with the inhibitor (1 μM) for 10 h. The xCELLigence system detects changes in impedance over time as the cells migrate to the electrode arrays on the bottom side of the upper chamber. Real-time cell invasion was monitored every 10 min for 60 h. Each sample was assayed in three or more replicates and repeated a minimum of three times to ensure reproducible trends were observed. A cell index of invasion was calculated using RTCA Software Package 1.2.

In vitro kinase assay and ADP-Glo kinase assay

SYK (Sigma-Aldrich, #S6448), cortactin (Abcam, Cambridge, United Kingdom, #ab131824), and cofilin (Abcam, #ab95396) recombinant proteins were phosphorylated in protein kinase buffer (New England Biolabs, Ipswich, MA, USA) with 100 μM ATP. The reactions were incubated at 37°C for 1 h, and the products were separated on SDS-PAGE gels. To estimate the amount of ADP produced in the kinase reactions, ADP-Glo Kinase

assay (Promega, Madison, WI, USA) was used according to the manufacturer's instructions. Luminescence generated by reactions performed in the absence of SYK were subtracted to eliminate any signal from background auto-phosphorylation of proteins.

3D double-layered tumor spheroid (3DLTS) invasion

A 3DLTS was made by mixing 10,000 cancer cells with 0.5 μl Matrigel (Corning, Bedford, MA, USA). The mixture was dropped into a spherical mold and incubated at 37°C for 30 minutes to allow gelation. The mixture was then harvested in fresh medium, and type I collagen solution (5 μl, Corning) was added to fully cover the Matrigel sphere containing cells. This mixture was then dropped into a spherical mold at 37°C for 1 hour to allow gelation of the type I collagen. The 3D double-layered tumor spheroid (3DLTS) was then harvested. A single 3DLTS was cultured as a suspension in a well, and time-lapse images were collected every day for 1 week using a Nikon TE2000 microscope (Nikon) equipped with a Cascade 1K CCD camera (Roper Scientific, Tucson, AZ, USA). To assess changes in cell numbers, the PrestoBlue assay (Thermo Fisher Scientific) was applied to the 3DLTS every 3 days. To quantify cell invasion, the 3DLTS was fixed with 4% paraformaldehyde and incubated with Hoechst33342 (1:2000, room temperature for 10 min; Thermo Fisher Scientific) and then processed for microscopic examination. Fluorescence images of the stained 3DLTS were acquired using a Nikon TE2000 microscope. Stained nuclei of cells from the inner sphere that had invaded were counted using ImageJ. Each sample was assayed in three or more replicates.

High-throughput cell-imaging platform (htCIP) immunostaining and fluorescence microscopy

Approximately 12,000 cells were plated in each well of a 24-well plate (MatTek, Ashland, MA, USA). After 24 h incubation, cells were fixed with 4% para-formaldehyde, permeabilized with Triton X-100 (Sigma-Aldrich), and blocked for nonspecific binding with 5% goat serum. Nuclear DNA was stained with DAPI, and actin was stained with either phalloidin Alexa Fluor 488 (Thermo Fisher Scientific) or Acti-stain 555 (Cytoskeleton Inc., Denver, CO, USA). For each sample, fluorescently labeled cells in seventy-two (8-by-9 square grid) fields of view from a low-magnification lens (10× Plan Fluor lens; N.A. 0.3, Nikon) with a CCD (Hamamatsu OCAR-ER) on a Nikon NI microscope covering a contiguous area of approximately 6.0 mm × 5.0 mm (30.0 mm^2) were analyzed. DAPI (nucleus) or phalloidin (F-actin) fluorescence was recorded to obtain morphometric information about the nucleus and cellular body of each cell within the scanning region. Segmentation of nuclear and cellular shape from images was conducted using a custom MATLAB code. At least 500 – 2500 cells/sample were analyzed for statistical analysis.

Total Internal Reflection Fluorescence (TIRF) Microscopy

Serum starved cells were infected with LifeAct-RFP and seeded at a low density on glass bottom plates. Total internal reflection fluorescence (TIRF) microscopy was carried out using a Nikon Eclipse TiE microscope illuminated by an Ar laser (GFP) and a diode laser (RFP). Images were acquired on a Photometrics Evolve EMCCD camera controlled by Nikon NIS-Elements. Actin dynamics were recorded at 30 sec per frame for 20 min. EGF (100 ng/mL) was added at the 5 min time point. To quantitatively measure actin protrusion

dynamics, we calculated the expanding regions of actin signal changes relative to the initial area for each time frame. At least 25 – 50 different fields, each containing a minimum of one cell/field were recorded per sample for adequate statistical analysis. The mean areas were measured after converting the images to binary format using ImageJ software.

Supplementary Material

Refer to Web version on PubMed Central for supplementary material.

Acknowledgments

This study was supported by NIH/NCI grants, RO1CA215483 (IMS), UO1CA200469 (IMS), RO1CA148826 (TLW), R21CA187512 (TLW), K22CA212060 (CHH) and KO1-CA166576 (MIV), Richard W. TeLinde Research Program (www.gynecologycancer.org), Ovarian Cancer Research Foundation Alliance (OCRFA) Grant # 458972 (IMS), The Honorable Tina Brozman Foundation (IMS &TLW), TEAL award (TLW), and US Department of Defense Ovarian Cancer Consortium grant W81XWH-11-2-0230 (IMS & TLW).

References

1. Bordeleau F, Alcoser TA, Reinhart-King CA. Physical biology in cancer. 5. The rocky road of metastasis: the role of cytoskeletal mechanics in cell migratory response to 3D matrix topography. Am J Physiol Cell Physiol. 2014; 306:C110–120. [PubMed: 24196535]
2. Yamaguchi H, Condeelis J. Regulation of the actin cytoskeleton in cancer cell migration and invasion. Biochim Biophys Acta. 2007; 1773:642–652. [PubMed: 16926057]
3. Hoon JL, Tan MH, Koh CG. The Regulation of Cellular Responses to Mechanical Cues by Rho GTPases. Cells. 2016:5.
4. Yap KL, Fraley SI, Thiaville MM, Jinawath N, Nakayama K, Wang J, et al. NAC1 Is an Actin-Binding Protein That Is Essential for Effective Cytokinesis in Cancer Cells. Cancer research. 2012; 72:4085–4096. [PubMed: 22761335]
5. Paz H, Pathak N, Yang J. Invading one step at a time: the role of invadopodia in tumor metastasis. Oncogene. 2014; 33:4193–4202. [PubMed: 24077283]
6. Hastie EL, Sherwood DR. A new front in cell invasion: The invadopodial membrane. Eur J Cell Biol. 2016; 95:441–448. [PubMed: 27402208]
7. Linder S, Wiesner C, Himmel M. Degrading devices: invadosomes in proteolytic cell invasion. Annu Rev Cell Dev Biol. 2011; 27:185–211. [PubMed: 21801014]
8. Yu Y, Gaillard S, Phillip JM, Huang TC, Pinto SM, Tessarollo NG, et al. Inhibition of Spleen Tyrosine Kinase Potentiates Paclitaxel-Induced Cytotoxicity in Ovarian Cancer Cells by Stabilizing Microtubules. Cancer Cell. 2015; 28:82–96. [PubMed: 26096845]
9. Mocsai A, Ruland J, Tybulewicz VL. The SYK tyrosine kinase: a crucial player in diverse biological functions. Nature reviews Immunology. 2010; 10:387–402.
10. Kurosaki T, Johnson SA, Pao L, Sada K, Yamamura H, Cambier JC. Role of the Syk autophosphorylation site and SH2 domains in B cell antigen receptor signaling. J Exp Med. 1995; 182:1815–1823. [PubMed: 7500027]
11. Tsang E, Giannetti AM, Shaw D, Dinh M, Tse JK, Gandhi S, et al. Molecular mechanism of the Syk activation switch. The Journal of biological chemistry. 2008; 283:32650–32659. [PubMed: 18818202]
12. Cheng S, Coffey G, Zhang XH, Shaknovich R, Song Z, Lu P, et al. SYK inhibition and response prediction in diffuse large B-cell lymphoma. Blood. 2011; 118:6342–6352. [PubMed: 22025527]
13. Young RM, Hardy IR, Clarke RL, Lundy N, Pine P, Turner BC, et al. Mouse models of non-Hodgkin lymphoma reveal Syk as an important therapeutic target. Blood. 2009; 113:2508–2516. [PubMed: 18981293]

14. Luangdilok S, Box C, Patterson L, Court W, Harrington K, Pitkin L, et al. Syk tyrosine kinase is linked to cell motility and progression in squamous cell carcinomas of the head and neck. Cancer research. 2007; 67:7907–7916. [PubMed: 17699797]
15. Lu J, Lin WH, Chen SY, Longnecker R, Tsai SC, Chen CL, et al. Syk tyrosine kinase mediates Epstein-Barr virus latent membrane protein 2A-induced cell migration in epithelial cells. The Journal of biological chemistry. 2006; 281:8806–8814. [PubMed: 16431925]
16. Prinos P, Garneau D, Lucier JF, Gendron D, Couture S, Boivin M, et al. Alternative splicing of SYK regulates mitosis and cell survival. Nat Struct Mol Biol. 2011; 18:673–679. [PubMed: 21552259]
17. Layton T, Stalens C, Gunderson F, Goodison S, Silletti S. Syk tyrosine kinase acts as a pancreatic adenocarcinoma tumor suppressor by regulating cellular growth and invasion. Am J Pathol. 2009; 175:2625–2636. [PubMed: 19893036]
18. Sharman J, Hawkins M, Kolibaba K, Boxer M, Klein L, Wu M, et al. An open-label phase 2 trial of entospletinib (GS-9973), a selective spleen tyrosine kinase inhibitor, in chronic lymphocytic leukemia. Blood. 2015; 125:2336–2343. [PubMed: 25696919]
19. Weinblatt ME, Kavanaugh A, Genovese MC, Musser TK, Grossbard EB, Magilavy DB. An oral spleen tyrosine kinase (Syk) inhibitor for rheumatoid arthritis. The New England journal of medicine. 2010; 363:1303–1312. [PubMed: 20879879]
20. Weinblatt ME, Kavanaugh A, Burgos-Vargas R, Dikranian AH, Medrano-Ramirez G, Morales-Torres JL, et al. Treatment of rheumatoid arthritis with a Syk kinase inhibitor: a twelve-week, randomized, placebo-controlled trial. Arthritis Rheum. 2008; 58:3309–3318. [PubMed: 18975322]
21. Friedberg JW, Sharman J, Sweetenham J, Johnston PB, Vose JM, Lacasce A, et al. Inhibition of Syk with fostamatinib disodium has significant clinical activity in non-Hodgkin lymphoma and chronic lymphocytic leukemia. Blood. 2010; 115:2578–2585. [PubMed: 19965662]
22. Lua BL, Low BC. Cortactin phosphorylation as a switch for actin cytoskeletal network and cell dynamics control. FEBS Lett. 2005; 579:577–585. [PubMed: 15670811]
23. Arber S, Barbayannis FA, Hanser H, Schneider C, Stanyon CA, Bernard O, et al. Regulation of actin dynamics through phosphorylation of cofilin by LIM-kinase. Nature. 1998; 393:805–809. [PubMed: 9655397]
24. Huang C, Liu J, Haudenschild CC, Zhan X. The role of tyrosine phosphorylation of cortactin in the locomotion of endothelial cells. The Journal of biological chemistry. 1998; 273:25770–25776. [PubMed: 9748248]
25. Yoo Y, Ho HJ, Wang C, Guan JL. Tyrosine phosphorylation of cofilin at Y68 by v-Src leads to its degradation through ubiquitin-proteasome pathway. Oncogene. 2010; 29:263–272. [PubMed: 19802004]
26. Wu PH, Phillip JM, Khatau SB, Chen WC, Stirman J, Rosseel S, et al. Evolution of cellular morpho-phenotypes in cancer metastasis. Scientific reports. 2015; 5:18437. [PubMed: 26675084]
27. Inagaki N, Katsuno H. Actin Waves: Origin of Cell Polarization and Migration? Trends Cell Biol. 2017; 27:515–526. [PubMed: 28283221]
28. Riedl J, Crevenna AH, Kessenbrock K, Yu JH, Neukirchen D, Bista M, et al. Lifeact: a versatile marker to visualize F-actin. Nat Methods. 2008; 5:605–607. [PubMed: 18536722]
29. Gagliardi PA, Puliafito A, di Blasio L, Chianale F, Somale D, Seano G, et al. Real-time monitoring of cell protrusion dynamics by impedance responses. Scientific reports. 2015; 5:10206. [PubMed: 25976978]
30. Xue L, Wang WH, Iliuk A, Hu L, Galan JA, Yu S, et al. Sensitive kinase assay linked with phosphoproteomics for identifying direct kinase substrates. Proc Natl Acad Sci U S A. 2012; 109:5615–5620. [PubMed: 22451900]
31. Pearce G, Audzevich T, Jessberger R. SYK regulates B-cell migration by phosphorylation of the F-actin interacting protein SWAP-70. Blood. 2011; 117:1574–1584. [PubMed: 21123826]
32. Ocana-Morgner C, Wahren C, Jessberger R. SWAP-70 regulates RhoA/RhoB-dependent MHCII surface localization in dendritic cells. Blood. 2009; 113:1474–1482. [PubMed: 18802007]
33. Beitz LO, Fruman DA, Kurosaki T, Cantley LC, Scharenberg AM. SYK is upstream of phosphoinositide 3-kinase in B cell receptor signaling. The Journal of biological chemistry. 1999; 274:32662–32666. [PubMed: 10551821]

34. Stephens LR, Anderson KE, Hawkins PT. Src family kinases mediate receptor-stimulated, phosphoinositide 3-kinase-dependent, tyrosine phosphorylation of dual adaptor for phosphotyrosine and 3-phosphoinositides-1 in endothelial and B cell lines. The Journal of biological chemistry. 2001; 276:42767–42773. [PubMed: 11524430]
35. Hatton O, Lambert SL, Krams SM, Martinez OM. Src kinase and Syk activation initiate PI3K signaling by a chimeric latent membrane protein 1 in Epstein-Barr virus (EBV)+ B cell lymphomas. PLoS One. 2012; 7:e42610. [PubMed: 22880054]
36. Moon KD, Post CB, Durden DL, Zhou Q, De P, Harrison ML, et al. Molecular basis for a direct interaction between the Syk protein-tyrosine kinase and phosphoinositide 3-kinase. The Journal of biological chemistry. 2005; 280:1543–1551. [PubMed: 15536084]
37. Yu L, Wang Y, Yao Y, Li W, Lai Q, Li J, et al. Eradication of growth of HER2-positive ovarian cancer with trastuzumab-DM1, an antibody-cytotoxic drug conjugate in mouse xenograft model. International journal of gynecological cancer : official journal of the International Gynecological Cancer Society. 2014; 24:1158–1164. [PubMed: 24987913]
38. Macdonald-Obermann JL, Pike LJ. Different epidermal growth factor (EGF) receptor ligands show distinct kinetics and biased or partial agonism for homodimer and heterodimer formation. The Journal of biological chemistry. 2014; 289:26178–26188. [PubMed: 25086039]
39. Li Y, Macdonald-Obermann J, Westfall C, Piwnica-Worms D, Pike LJ. Quantitation of the effect of ErbB2 on epidermal growth factor receptor binding and dimerization. The Journal of biological chemistry. 2012; 287:31116–31125. [PubMed: 22822073]
40. Cox D, Chang P, Kurosaki T, Greenberg S. Syk tyrosine kinase is required for immunoreceptor tyrosine activation motif-dependent actin assembly. The Journal of biological chemistry. 1996; 271:16597–16602. [PubMed: 8663235]
41. Jaumouille V, Farkash Y, Jaqaman K, Das R, Lowell CA, Grinstein S. Actin cytoskeleton reorganization by Syk regulates Fcgamma receptor responsiveness by increasing its lateral mobility and clustering. Dev Cell. 2014; 29:534–546. [PubMed: 24914558]
42. Coopman PJ, Do MT, Barth M, Bowden ET, Hayes AJ, Basyuk E, et al. The Syk tyrosine kinase suppresses malignant growth of human breast cancer cells. Nature. 2000; 406:742–747. [PubMed: 10963601]
43. Ghotra VP, He S, van der Horst G, Nijhoff S, de Bont H, Lekkerkerker A, et al. SYK is a candidate kinase target for the treatment of advanced prostate cancer. Cancer research. 2015; 75:230–240. [PubMed: 25388286]
44. Zhang X, Shrikhande U, Alicie BM, Zhou Q, Geahlen RL. Role of the protein tyrosine kinase Syk in regulating cell-cell adhesion and motility in breast cancer cells. Molecular cancer research : MCR. 2009; 7:634–644. [PubMed: 19435818]
45. Ruschel A, Ullrich A. Protein tyrosine kinase Syk modulates EGFR signalling in human mammary epithelial cells. Cellular signalling. 2004; 16:1249–1261. [PubMed: 15337524]
46. Kurman RJ, Shih Ie M. The Dualistic Model of Ovarian Carcinogenesis: Revisited, Revised, and Expanded. Am J Pathol. 2016; 186:733–747. [PubMed: 27012190]
47. Kunwar S, Devkota AR, Ghimire DK. Fostamatinib, an oral spleen tyrosine kinase inhibitor, in the treatment of rheumatoid arthritis: a meta-analysis of randomized controlled trials. Rheumatol Int. 2016
48. Pohl G, Ho CL, Kurman RJ, Bristow R, Wang TL, Shih Ie M. Inactivation of the mitogen-activated protein kinase pathway as a potential target-based therapy in ovarian serous tumors with KRAS or BRAF mutations. Cancer research. 2005; 65:1994–2000. [PubMed: 15753399]
49. Ran FA, Hsu PD, Wright J, Agarwala V, Scott DA, Zhang F. Genome engineering using the CRISPR-Cas9 system. Nat Protoc. 2013; 8:2281–2308. [PubMed: 24157548]

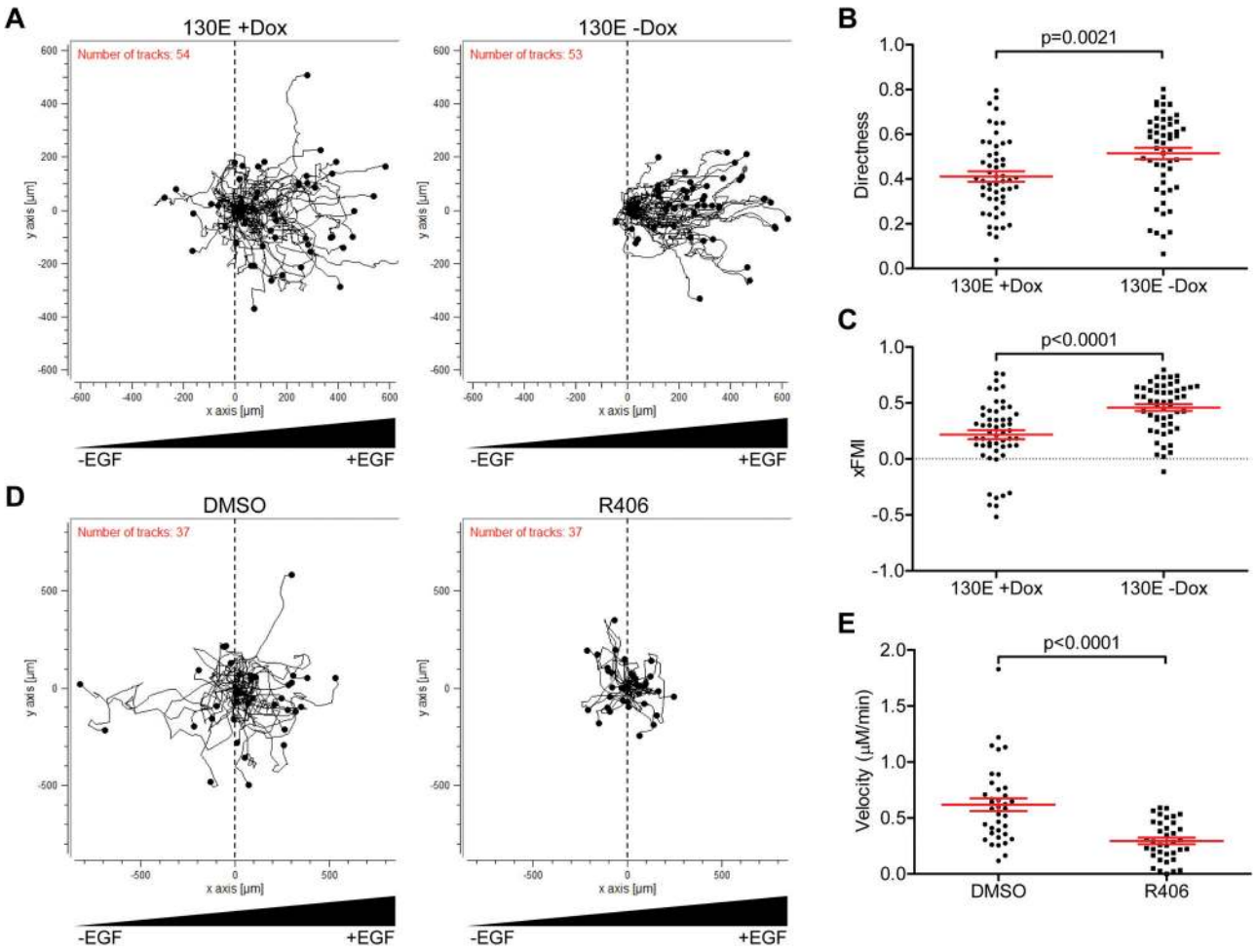

Figure 1.

Expression of active SYK increases directed migration toward increasing EGF. **A–C.** Trajectories of SKOV3 cells seeded into EGF gradients on chemotaxis microscope slides. **A**. (*left*) Migration in the absence of active SYK^{130E} (+Dox). (*right*) Migration in the presence of constitutively active SYK^{130E} mutant (−Dox). **B**. Scatter plot quantitation of EGF-directed cell movement. **C**. Scatter plot quantitation of xFMI (x-axis Forward Migration Index). **D.** Trajectories of SKOV3 cells in EGF gradients in the presence of solvent (DMSO) control (*left*) or in the presence of SYK inhibitor (R406) (*right*). **E.** Scatter plot quantitation of R406 effects on the velocity of cell movement. Results are shown as mean ± SEM. Statistical evaluation were performed using two-tailed Mann-Whitney test.

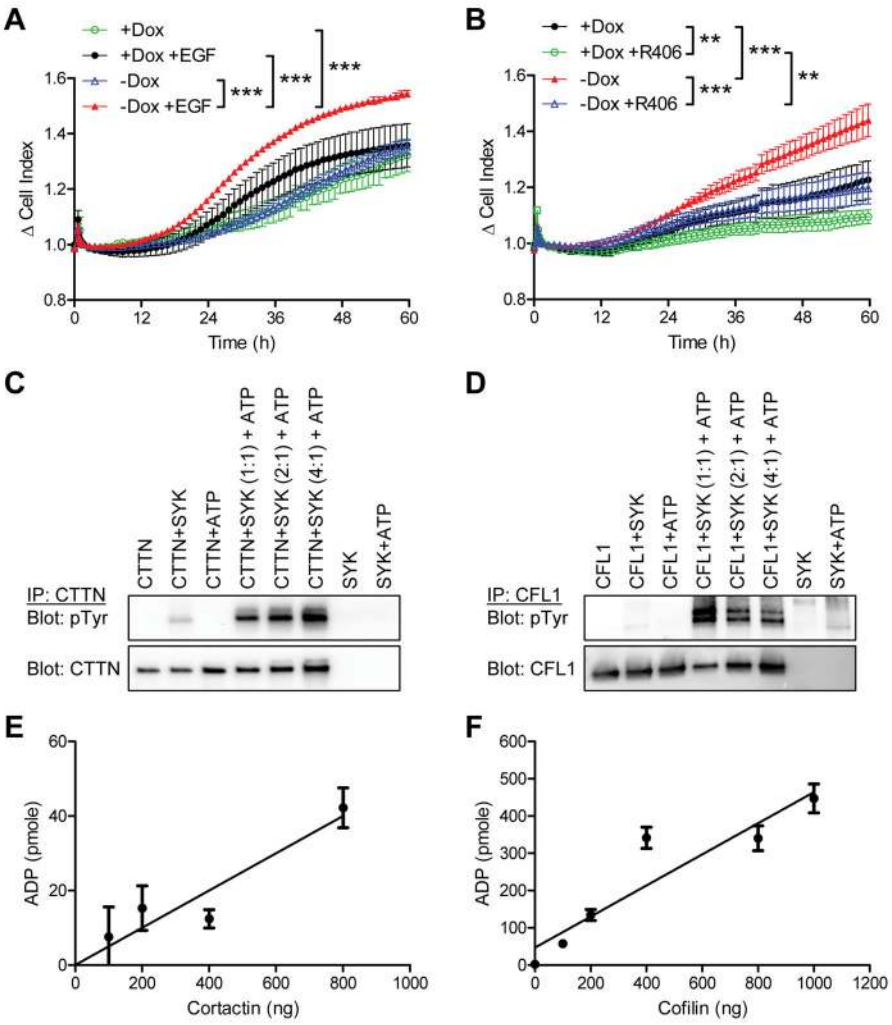

Figure 2.

Real-time invasion measurement of SKOV3 cells expressing SYK^{130E} active mutant under a Tet-off inducible system using xCELLigence cell impedance assay. **A.** SYK^{130E} mutant expressing cells (−Dox) and non-expressing cells (+Dox) were studied. EGF (25 ng/mL) was used as a chemoattractant in the lower chamber. Cells were serum starved prior to the experiment. Cell index data were set to read at 10 minute intervals over the course of 60 h. Plots represent data collected at one-hour time points. **B.** Similar experiments were performed under treatment with R406 (1 μM); all conditions in this plot had EGF in the lower chamber. Results are shown as mean ± SEM. **p<0.01; ***p<0.001 as determined by one-way ANOVA with Bonferroni's multiple comparison post-test by comparing two groups over time. **C.** *In vitro* kinase assay using recombinant active SYK and cortactin (CTTN) in the presence or absence of ATP. Following kinase reactions, proteins were immunoprecipitated using an anti-CTTN antibody, and were analyzed by Western blot probed with an antibody specific for phosphotyrosine (pTyr). Total CTTN was included as a loading control. **D.** *In vitro* kinase reactions as in (C) performed using recombinant active SYK and cofilin-1 (CFL1) proteins. **E–F.** ADP-Glo kinase assay to quantify ADP

production in the *in vitro* kinase reactions by active recombinant SYK with CTTN or CFL1 proteins. Results are shown as mean ± SEM.

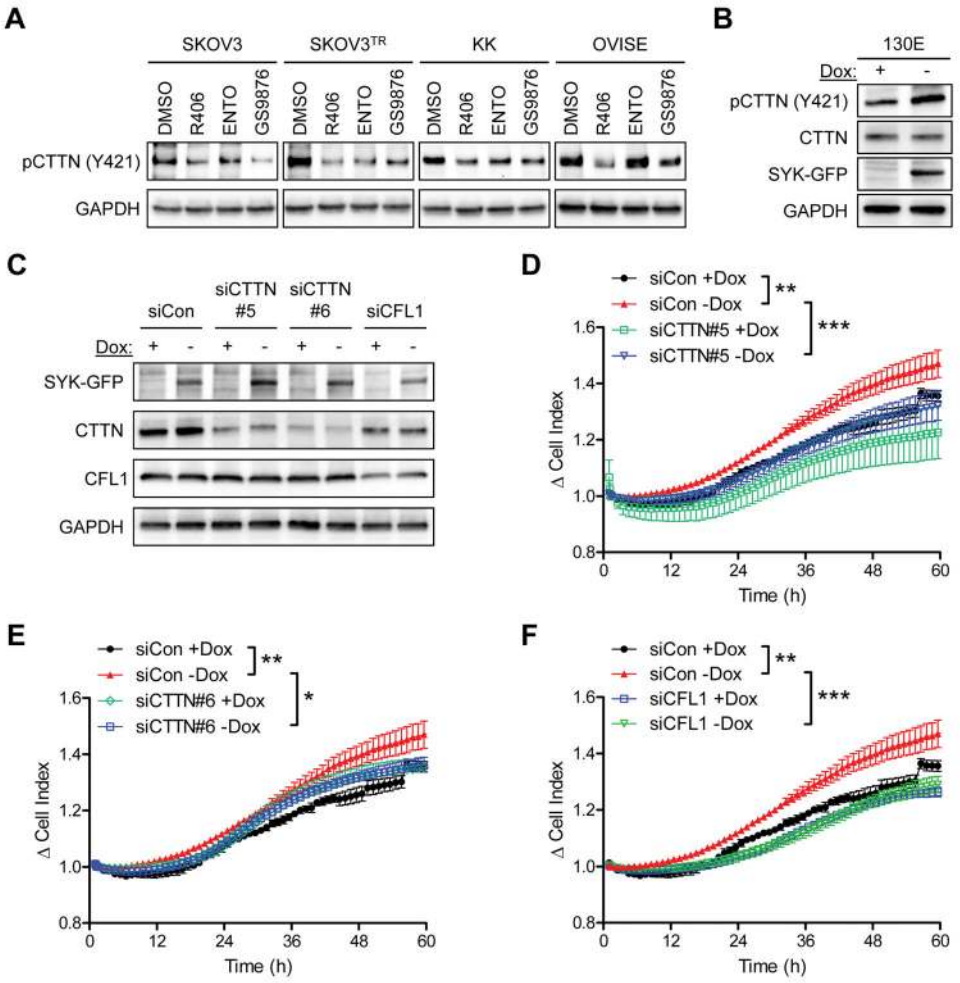

Figure 3.

Involvement of cortactin in SYK-mediated invasion. **A.** Phosphorylation of CTTN (Y421) in a panel of ovarian cancer cell lines (SKOV3, SKOV3^{TR}, KK, and OVISE) after incubation with SYK inhibitors R406, ENTO (Entospletinib), or GS9876 (all at 700 nM) for 24 h. GAPDH is used a loading control. **B.** Western blot analysis of pCTTN (Y421) expression in SKOV3 cells expressing SYK^{130E} active mutant (−Dox). **C.** Western blot analysis of SKOV3 SYK^{130E} cells transfected with control siRNA (siCon), CTTN siRNAs (siCTTN#5 or siCTTN#6), or CFL1 siRNA (siCFL1). **D–F.** Real-time invasion measurement of siRNA transfected SKOV3 SYK^{130E} cells with EGF in the lower chamber. Results are shown as mean ± SEM. *p<0.05; **p<0.01; ***p<0.001 as determined by one-way ANOVA with Bonferroni's multiple comparison post-test by comparing two groups over time.

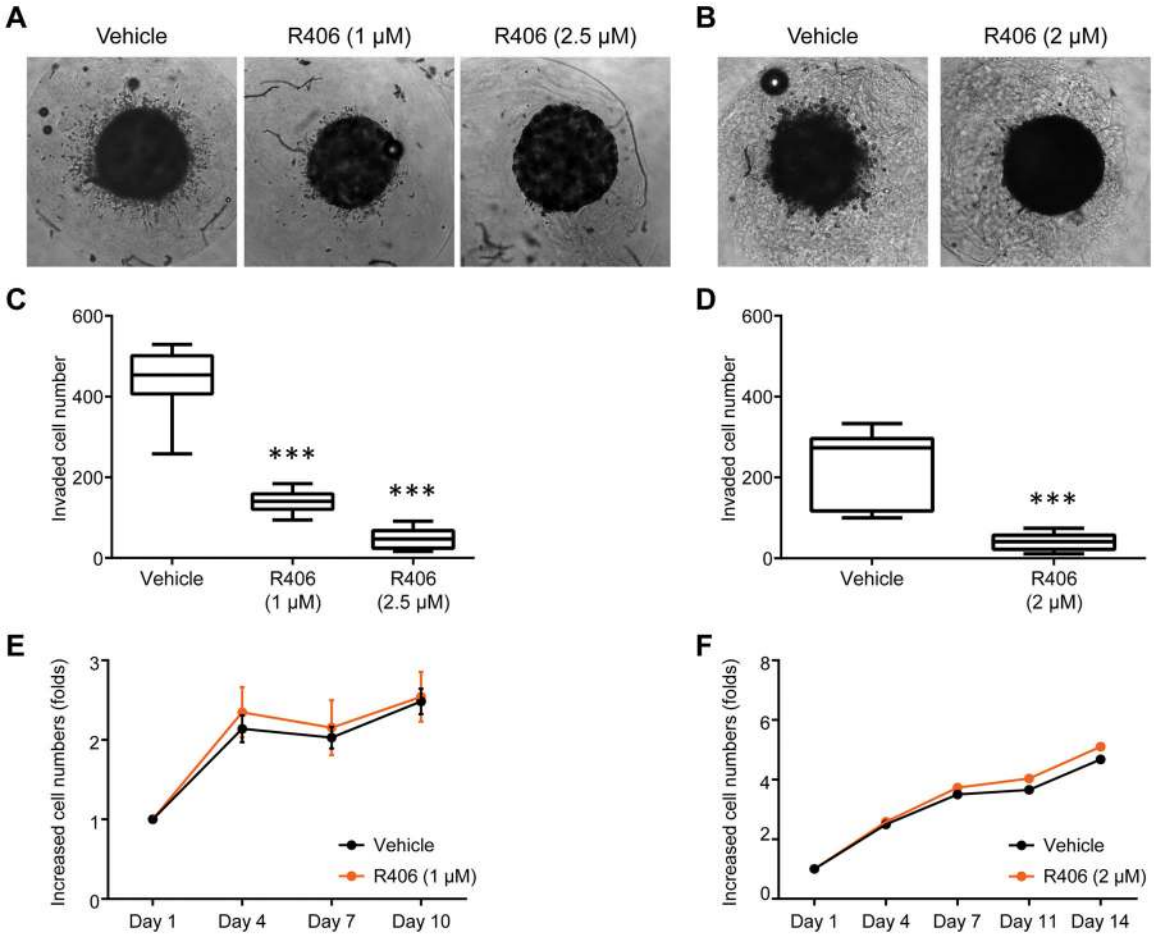

Figure 4.

R406 reduces tumor cell invasion in a 3D spheroid invasion assay. **A and B.** Representative images of SKOV3 (A) and OVISE (B) tumor spheroids treated with vehicle (DMSO) or R406 at the indicated concentrations. **C.** The quantitation of invading SKOV3 cells. Cells were stained using Hoechst33342 and analyzed using ImageJ software. **D.** Similar analysis for invading cells performed with OVISE spheroids. **E and F.** Cell viability determined by PrestoBlue to determine the effect of R406 on proliferation of SKOV3 (E) and OVISE (F) cells in spheroids. Results are shown as mean ± SD. ***p<0.001 as determined by one-way ANOVA.

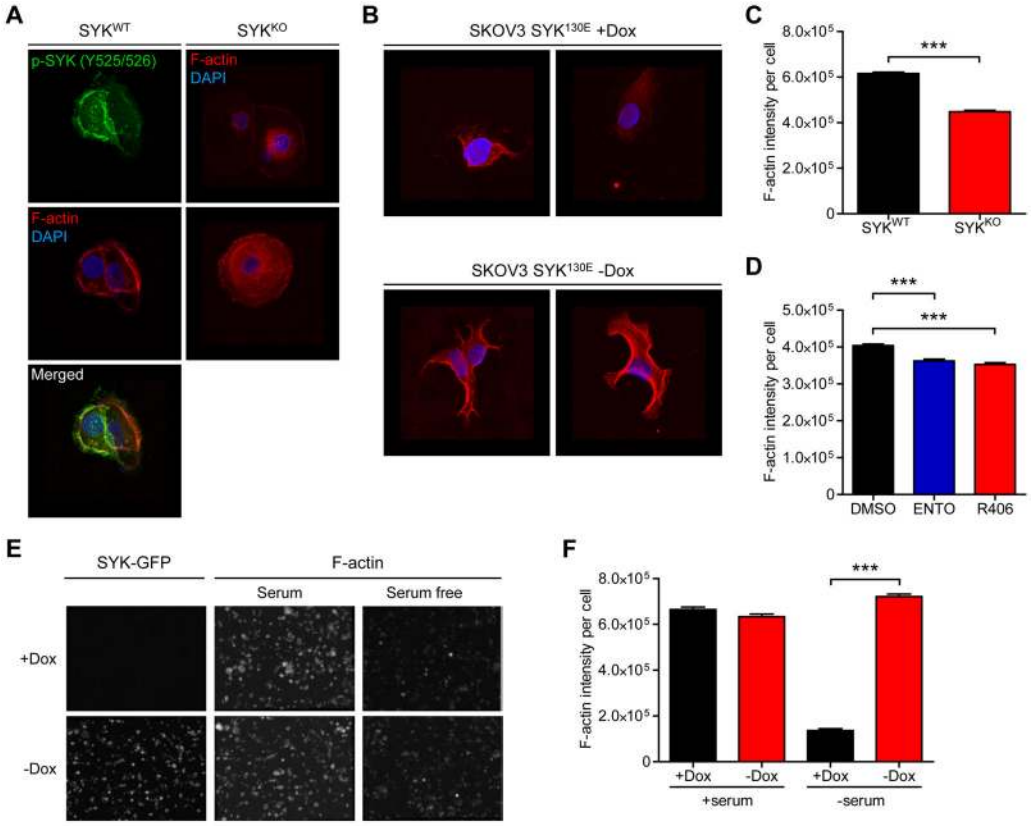

Figure 5.

SYK modulation affects cortical F-actin intensity. **A.** Confocal images of immunofluorescence staining in OVISE SYK^{WT} cells (one representative field) and OVISE SYK^{KO} cells (two representative fields). Red fluorescence: F-actin stained with phalloidin; blue fluorescence: DAPI (nuclei); green fluorescence: pSYK(Y525/526). **B.** SKOV3 cells expressing SYK^{130E} active mutant (−Dox). Two representative fields are shown for each condition. **C.** SYK knockdown reduces overall F-actin intensity in cells. F-actin fluorescence signal was determined in SYK^{WT} and SYK^{KO} OVISE cells. Results are shown as mean ± SEM. *** $p<0.001$ as determined using two-tailed Mann-Whitney test. **D.** Effect on F-actin intensity of SYK inactivation by inhibitors ENTO (Entospletinib) or R406 (both at 700 nM) for 24 h in $MPSC1^{TR}$ cells. **E.** Representative F-actin fluorescence images from SKOV3 cells expressing SYK^{130E} active mutant (−Dox). **F.** Effect of ectopic expression of active SYK (−Dox) on F-actin intensity in serum free medium. F-actin intensity per cell was measured using a high-throughput cell-imaging platform (htCIP). Results are shown as mean ± SEM. ***$p<0.001$ as determined by one-way ANOVA followed by Dunn's multiple comparison post hoc test.

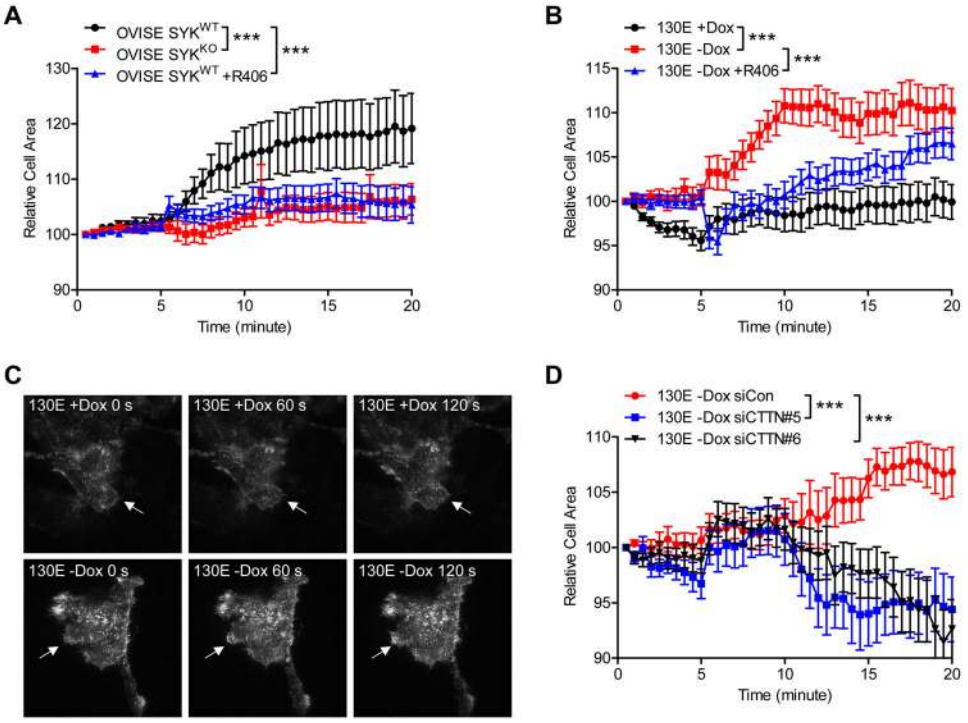

Figure 6.

SYK activity affects EGF-induced actin protrusion dynamics examined by TIRF microscopy. **A.** OVISE SYK^{WT} and SYK^{KO} cells were infected with LifeAct-RFP and serum starved overnight prior to imaging by TIRF microscopy. Cells were imaged at 30 sec intervals over a 25 min time period (Video S1–3). Cells were stimulated with 100 ng/ml EGF at the 5 min time point. Quantitative data on cell surface area variation (as determined from the actin-RFP signal) observed with EGF stimulation are shown relative to the original unstimulated cell surface prior to addition of EGF. To measure SYK inhibition, OVISE SYK^{WT} cells were treated with R406 (700 nM) for 24 h prior to the experiment. **B.** SKOV3 cells expressing SYK^{130E} active mutant (−Dox) were imaged under TIRF microscopy using similar conditions as in (A) (Video S4–6). **C.** Representative images of actin protrusion by SKOV3 SYK^{130E} non-induced (+Dox) and induced (−Dox) cells. **D.** SKOV3 cells expressing SYK^{130E} were transfected with either control siRNA (siCon) or siRNAs for CTTN (siCTTN) and were treated and imaged as in panels A and B. Results are shown as mean ± SEM. ***$p<0.001$ as determined by one-way ANOVA with Bonferroni's multiple comparison post-test by comparing two groups over time.